

Numerical Simulation of Particle Capture by Circular Cylinders

A. Espinosa^{1,2}, M. Ghisalberti¹, G. Ivey^{1,2} and N. Jones^{1,2}

¹School of Environmental Systems Engineering
 University of Western Australia, Western Australia 6009, Australia

²UWA Oceans Institute
 University of Western Australia, Western Australia 6009, Australia

Abstract

The capture of suspended particles by vegetation is an important mechanism in many aquatic processes. In order to better understand particle capture dynamics, a numerical model was set up to simulate the 2D flow of particle-laden fluid around cylindrical obstacles.

Numerical results show that the capture efficiency increases with the Reynolds number and with the particle size, in good agreement with the laboratory experiments of Palmer *et al.* [9].

Our results show that captured particles originate from a much wider area upstream than previously thought and, counterintuitively, particles directly upstream of the centre of the cylinder are not the most likely to be captured.

Introduction

Aquatic vegetation (such as reeds, seagrass and kelp) is a critical component of many ecosystems and can dramatically improve water quality and ecological function by the capture of different kinds of particles. Aquatic vegetation is typically coated by a thin, sticky biofilm, rendering it efficient at capturing particles in suspension (e.g. sediment, larvae and pollen). This particle capture can increase water clarity, impact water quality through the removal of adsorbed pollutants and play a key role in the breeding cycles of many species. Despite this fundamental importance, little is known about the efficiency of particle capture by aquatic vegetation, nor the impact of stem wakes upon this overall capture process.

Many studies have reported theoretical, experimental and numerical analyses of particle capture by cylindrical collectors. However, the majority of these studies have focused on aerosols [3,4,12,13]. The results from these studies cannot be applied to particle capture by aquatic vegetation due to significant differences in key parameters such as the Reynolds number, Stokes number and the ratio of particle density to fluid density. In order to better understand particle capture by aquatic vegetation, we used a numerical model to simulate the 2-D flow of particle-laden fluid around cylindrical obstacles. The experimental measurements of Palmer *et al.* [9], in a parameter space relevant to aquatic vegetation, were used to validate the numerical simulations.

Fundamental Equations and Methodology

Fluid flow governing equations

The 2-D continuity and Navier-Stokes equations were solved for incompressible unsteady laminar flow past a circular cylinder. Using the cylinder diameter D and the uniform inlet velocity U_∞ as the length and velocity scales, respectively, and the advective time scale $\tau_f = D/U_\infty$ for nondimensionalizing these equations we get

$$\frac{\partial u_i}{\partial x_i} = 0, \quad (1)$$

$$\frac{\partial u_i}{\partial t} + u_j \frac{\partial u_i}{\partial x_j} = -\frac{\partial p}{\partial x_i} + \frac{1}{Re} \frac{\partial^2 u_i}{\partial x_j \partial x_j}. \quad (2)$$

Here the Reynolds number is defined as $Re = \rho U_\infty D / \mu$, ρ is the fluid density, μ is the fluid absolute viscosity, p is the non-dimensional pressure, u_i is the non-dimensional fluid velocity, t is the non-dimensional time and x_i are the non-dimensional coordinates. Gravity was not considered as it acts perpendicular to the plane of the 2-D simulation.

Computational scheme and domain

The flow of particle-laden fluid past a single circular cylinder was solved in a 2-D configuration. The centre of the cylinder was at the origin of a domain with dimensions $L_i = 30D$, $L_o = 30D$, $L_b = 30D$, $H = 2L_b$ (see figure 1). The flow entered the domain at $x = -L_i/D$ with a uniform, unidirectional non-dimensional velocity, $u_x = 1$.

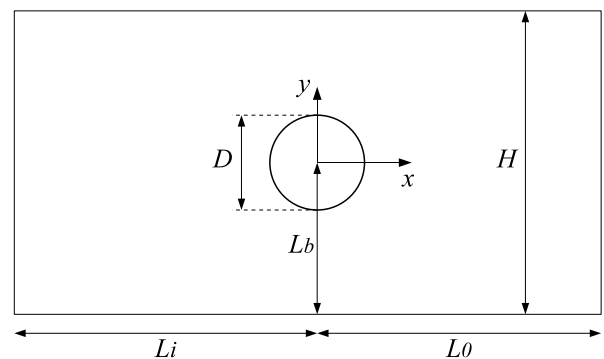


Figure 1. Definition of computational domain.

We used the computational fluid dynamics code, OpenFOAM [10], to solve the fluid and the particle dynamics. Equations (1) and (2) were discretized using a finite-volume approach on an unstructured grid. A second-order scheme in space was used for spatial derivatives and interpolations. The pressure-velocity coupling was solved using the PIMPLE scheme included in OpenFOAM. Time integration was achieved with a second-order two-time-level scheme, using maximum Courant numbers of approximately 0.25.

The domain configuration and boundary conditions agreed with the guidelines proposed by Posdziech and Grundmann in order to avoid considerable blockage effects [11]. A no-slip boundary condition was set for the cylinder wall, and a fine grid resolution was used close to the cylinder to resolve the boundary layer.

The code was validated against experimental data [8,14] and direct numerical solutions [11]. The Reynolds number dependencies of the vortex shedding frequency and the drag, lift and pressure coefficients were all captured accurately (to within 2% of error).

Particle Dynamics Equation

The particles in the flow were assumed to be spherical, with a low particle Reynolds number ($Re_p = \rho u_{rel} d_p / \mu$, where u_{rel} is the velocity of the particle relative to the surrounding fluid and d_p is the particle diameter). The particles were assumed not to affect the fluid flow and not to interact with each other. A simplified version of the Basset-Boussinesq-Ossen (BBO) equation [1,2,7] was used to simulate the particle dynamics. Barton [1] showed that for very low Stokes number, the steady drag force is the dominant force term in the BBO equation, being two orders of magnitude greater than all other terms.

The Stokes number is defined as

$$S = \frac{\tau_p}{\tau_f} = \frac{d_p^2 \rho_p U_\infty}{18 \mu D} = \frac{1}{18} R^2 \varepsilon Re \quad (3)$$

where τ_p is the particle response time, ρ_p is the particle density, $R = d_p/D$ is the diameter ratio and $\varepsilon = \rho_p/\rho$ is the density ratio [3].

As our applications have a very low Stokes number (less than 6×10^{-3}), we calculated particle trajectories using only the steady drag force. The simplified BBO equation can be written in non-dimensional form as

$$\frac{d^2 x_{pi}}{dt^2} = \frac{du_{pi}}{dt} = -C_{DS} \frac{u_{pi} - u_i}{S} \quad (4)$$

where x_{pi} is the particle position, u_{pi} is the particle velocity and C_{DS} is the correction for the steady state drag coefficient [2] given by

$$C_{DS} = 1 + \frac{1}{6} Re_p^{2/3} \quad (5)$$

Definition of capture efficiency

The capture efficiency η is defined as the ratio of the number of particles captured by the cylinder (n_c) to the number of particles N that entered the domain through a window defined by the upstream projected area of the cylinder (i.e. in the range $-D/2 \leq y \leq D/2$),

$$\eta = \frac{n_c}{N} \quad (6)$$

Assuming that the particles enter the domain with the same uniform velocity as the fluid, N can be calculated for a given duration T by

$$N = PDhTU_\infty \quad (7)$$

where P is the particle concentration and h is the length of the cylinder in the spanwise direction.

It is typically thought that all the captured particles enter the domain within a narrow window of width b centred at $y=0$, such that the capture efficiency can be defined by a width ratio as

$$\eta_w = \frac{b}{D} \quad (8)$$

The width of this narrow window is usually estimated using the same principle as equation (7), considering only the number of captured particles:

$$n_c = PbhTU_\infty \quad (9)$$

Our results show that the captured particles come from a window of width B that is much bigger than b estimated from equations (8) or (9). The definition of capture efficiency from equation (6) is more fundamental and is the one used in this work.

Lagrangian algorithm for particle trajectories

Fluid flow simulations were run until the flow was fully developed and stable vortex shedding frequencies were established. Particles were then injected into the domain at the inlet ($x=-L_i$) with a velocity equal to that of the fluid ($u_p=U_\infty$). The injection duration T was equal to two vortex shedding periods and the particles were tracked until they had either been captured or bypassed the cylinder completely. The particles were injected at concentrations ranging from 3.81×10^5 to 1.66×10^7 [particles/D²].

The modified BBO equation (4) was integrated for each particle using the exponential Euler scheme [5]. As the particle positions did not coincide with the grid points, a second order interpolator was used to obtain the fluid velocity at the particle locations. Particles were captured when the distance from the particle centre to the cylinder wall was less than or equal to the particle radius. The collector was considered 'perfect' in the sense that every particle that touched the cylinder was captured.

Results

Particle capture efficiency

Several numerical experiments were performed, with large ranges of Reynolds number ($38 \leq Re \leq 486$) and diameter ratio R ($0.008 \leq R \leq 0.031$). Figure 2 compares the numerical capture efficiencies to the experimental measurements of Palmer *et al.* [9]. As in Palmer *et al.* [9], the density ratio was held constant ($\varepsilon=1.03$).

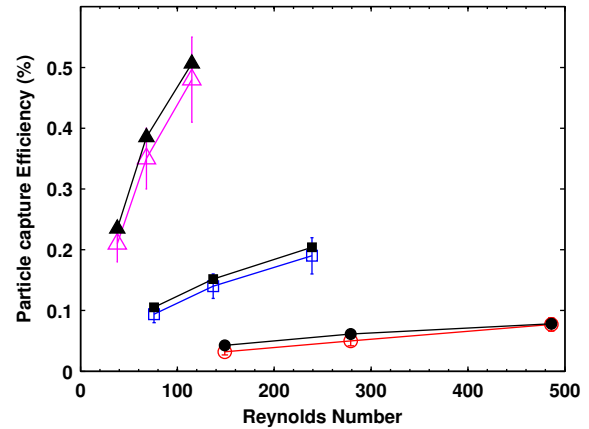


Figure 2. Particle capture efficiency as a function of Reynolds number. The coloured curves are the experimental results of Palmer *et al.* [9]. (○):R=0.008. (□):R=0.015. (△):R=0.031. The black curves are the numerical results of this study. (●):R=0.008. (■):R=0.015. (▲):R=0.031. The numerical and experimental results agree very well (to within 9% of error, on average).

As seen in figure 2, the numerical model predicted the magnitude of particle capture, and its variation with Reynolds number, excellently over the range of Reynolds numbers and diameter ratios tested. The numerical capture efficiencies were consistently higher than the experimental data, but were within the experimental confidence intervals based on the propagated uncertainty for one trial [9] (shown by the error bars in figure 2). The likely cause of this discrepancy is the assumption of the model cylinder being a perfect collector, which may not hold in the experiments of Palmer *et al.* [9].

The effect of oscillations in the flow

For $Re > 49$ the flow past a circular cylinder becomes unsteady and vortex shedding appears in the wake [11]. Unsteady conditions for pressure and velocity fields prevail in the vicinity of the cylinder, even on the upstream face [6]. Oscillations upstream of the cylinder cause particle capture to be much more complex than the typical conceptual model based on a perfectly steady upstream velocity.

Our simulations demonstrated that the upstream oscillations, which were in phase with the downstream vortex shedding, caused the particles to move laterally, thereby increasing the effective lateral extent of the window B from which captured particles enter the domain. In order to show how particles paths were influenced by these upstream oscillations, a series of snapshots of the particle positions as they move towards the cylinder is shown in figure 3. The Reynolds number and particle diameter ratio were 115 and 0.031, respectively. For visualisation purposes, only a thin strip of particles with an injection y coordinate of $\pm 0.0025D$ is shown. The colour contours show the value of the x -component of the fluid velocity. Oscillations on the lee side of the cylinder are easily detectable by observing the changes in the fluid velocity field, while oscillations on the upstream face were more subtle, but can be identified by the particle trajectories.

In figure 3(a), an instantaneously positive lateral velocity immediately upstream of the cylinder caused all particles in the thin strip to be diverted around one side ($y > 0$) of the cylinder. As the lateral component of the velocity upstream of the cylinder reversed direction (figure 3(b)), particles in the strip were diverted around the other side of the cylinder ($y < 0$), creating a bend in the particle strip. The particles that were not captured were advected past the cylinder and began to be influenced by the cylinder wake (figure 3(c)) while the approaching particles on the upstream side were again diverted to the positive y side.

As explained above, the lateral extent B of the window from which captured particles come was much greater than the value of b estimated from equations (8) or (9). Figure 4 shows a histogram of the injection y coordinates of the captured particles for a simulation with $Re=149$ and $R=0.008$. The number of particles injected within each interval of the histogram was 1371. For these conditions, the numerical capture efficiency was 0.00042, resulting in $b=0.00042D$ while $B=0.034D$: 80 times greater.

Clearly, not all of the particles injected within $-B/2 < y < B/2$ were captured. Surprisingly, the particles least likely to be captured are those initially near the symmetry plane $y=0$, with a probability of capture of 0.95%. In summary, our simulations demonstrate that oscillations in the flow around the cylinder invalidate the concept of a thin upstream capture zone of width b within which all particles are captured by the cylinder. Rather, we found that the upstream capture zone is much wider than b ; all particles within this broad capture zone had a likelihood of capture that was in the range from 1 to 7%.

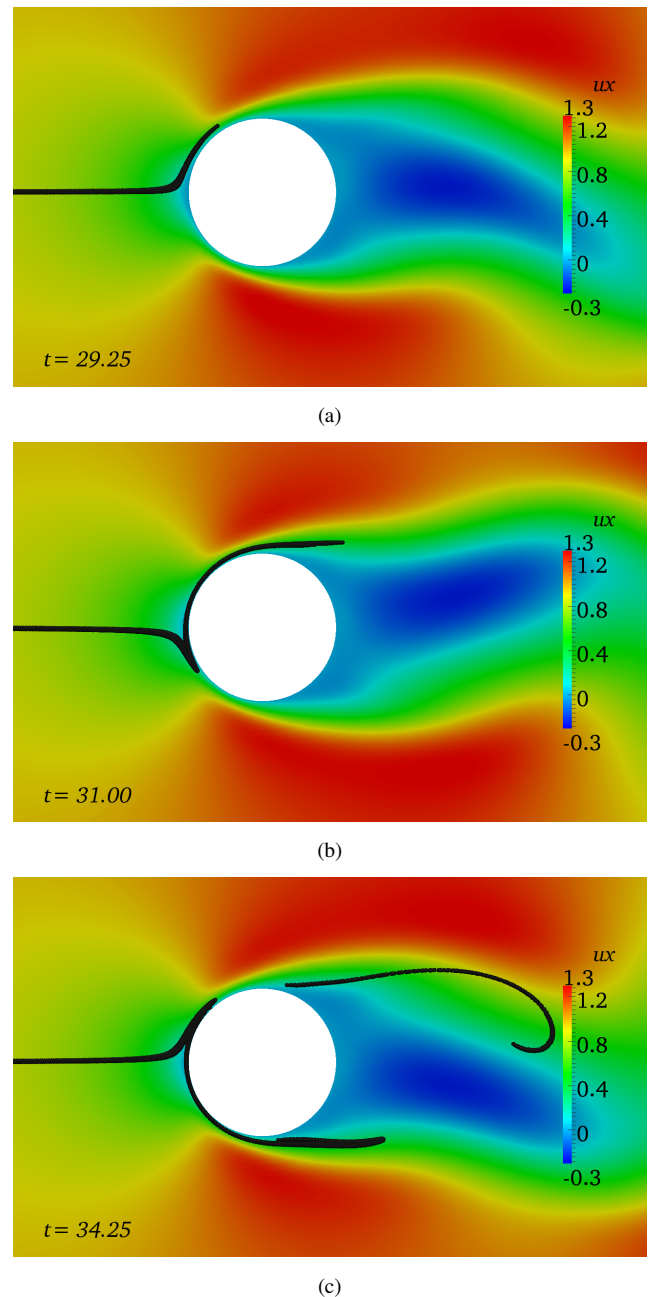


Figure 3. Series of snapshots of particle positions for $Re=115$, $R=0.031$. Particles are shown in black. Individual particles are not seen because of the high particle concentration in the strip. Colour contours indicate the magnitude of the x -component of the non dimensional fluid velocity. The non-dimensional time measured from the beginning of the simulation is also shown in each snapshot.

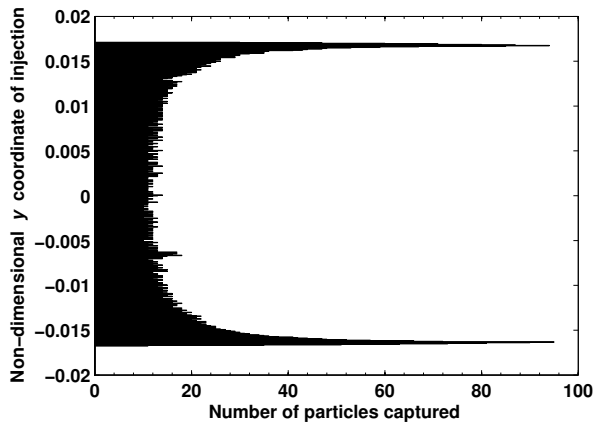


Figure 4. Histogram of the number of particles captured according to their non-dimensional y coordinate of injection ($Re=149$, $R=0.008$). The number of initial particles injected within each y -interval was 1371.

Conclusions

We used a 2-D particle-laden fluid flow model to predict the capture of suspended particles by cylindrical collectors. In comparison to experimental measurements, capture efficiency and its variation with Reynolds number and particle size were well predicted. As prediction of capture efficiencies for aquatic vegetation is extremely limited, the model is a very valuable tool for evaluating particle-vegetation interaction in aquatic systems.

Acknowledgements

A. Espinosa acknowledges the scholarships granted by CONACyT, Mexico and The University of Western Australia.

References

- [1] Barton, I.E., Computation of Particle Tracks over a Backward-Facing Step, *J. Aerosol Sci.*, **26**, 1995, 887-901.
- [2] Brandon D.J. and Aggarwal S.K., A Numerical Investigation of Particle Deposition on a Square Cylinder Placed in a Channel Flow, *Aerosol Sci. Tech.*, **34**, 2001, 340-352.
- [3] Fuchs N.A., *The Mechanics of Aerosols*, Pergamon Press, 1964.
- [4] Hinds, W.C., *Aerosol Technology*, John Wiley & Sons, 1999.
- [5] Hockbruck, M., Lubich, C. and Selhofer, H., Exponential Integrators for Large Systems of Differential Equations. *SIAM J. Sci. Comput.*, **19**, 1998, 1552-1574.
- [6] Isaev, S.A., Leontiev, A.I., Kudryavtsev, N.A., Baranova, T.A. & Lysenko, D.A., Numerical Simulation of Unsteady-State Heat Transfer under Conditions of Laminar Transverse Flow Past a Circular Cylinder, *High Temperature*, **43**, 2005, 746-759.
- [7] Maxey, R.M. & Riley, J.J., Equation of Motion for a Small Rigid Sphere in a Non-Uniform Flow, *Phys. Fluids*, **25**, 1983, 883-889.
- [8] Norberg C., Fluctuating Lift on a Circular Cylinder: Review and New Measurements, *J. Fluids Struct.*, **17**, 2003, 57-96
- [9] Palmer, M.R., Nepf, H.M., Petterson, T.J.R. & Ackerman, J.D., Observations of Particle Capture on a Cylindrical Collector: Implications for Particle Accumulation and Removal in Aquatic Systems, *Limnol. Oceanogr.*, **49**, 2004, 76-85.
- [10] OpenFOAM, (<http://www.openfoam.com/>), 2010.
- [11] Posdziech, O. & Grundmann, R., A Systematic Approach to the Numerical Calculation of Fundamental Quantities of the Two-dimensional Flow over a Circular Cylinder, *J. Fluids Struct.*, **23**, 2007, 479-499.
- [12] Temu, A.K., Naess, E. & Sonju, O.K., Experimental Study of Particle Deposition onto a Cylinder in Crossflow, in *International Conference on Mitigation of Heat Exchanger Fouling and Its Economic and Environmental Implications*, 2001, 401-408.
- [13] Wessel, R.A. & Righi, J., Generalized Correlations for Inertial Impaction of Particles on a Circular Cylinder, *Aerosol Sci. Tech.*, **9**, 1988, 29-60.
- [14] Williamson, C.H.K., Advances in our Understanding of Vortex Dynamics in Bluff Body Wakes, *J. Wind Eng. Ind. Aerod.*, **71**, 1997, 3-32.